

Transport properties of sorbing contaminants in a fractured granite under oxidizing conditions

Chung-Kyun Park[†], Won-Jin Cho and Pil-Soo Hahn

Research Team of High Level Radioactive Waste Disposal, Korea Atomic Energy Research Institute,
Yousung P.O. box 105, Daejeon 305-600, Korea
(Received 13 December 2005 • accepted 25 April 2006)

Abstract—Migration of some sorbing chemical species has been studied in a single rock fracture of 1 m scale in order to understand the transport behavior of contaminants at underground environments. For the tracers, tritium and anions were used as nonsorbing ones and some sorbing cations such as Sr, Co and Cs were used as well. The experimental study was focused on the identification of the retardation and matrix diffusion of the tracer in the fracture. The hydraulic conductivity in the fracture was determined from the pressure differentials between pairs of boreholes. The hydraulic data were used with a variable aperture channel model to characterize the aperture distribution in the fracture. A transport model has been developed to describe the migration of the solutes in the flow field by using a particle tracking method. Results were plotted in the form of elution curves and migration plumes in the fracture. The experimental elution curves have been explored with the transport model which takes into account sorption and diffusion into the rock matrix. This comparison may contribute to further understanding on the heterogeneous flow field and the interactions between rock and chemical species.

Key words: Transport, Sorption, Matrix Diffusion, Retardation, Particle Tracking Method, Distribution Coefficient

INTRODUCTION

Isolating toxic wastes from the biosphere is becoming an important social and technical issue. Many countries are running or planning repositories for the wastes including radioactive ones. Usually, hazardous wastes are disposed in a trench type concrete block in shallow land, while radioactive wastes are considered to be disposed in deep hardrock mass. In order to assess whether the waste is sufficiently segregated from the biosphere, the characteristics of geologic media around the repository as well as interactions among wastes, groundwater, and geomedia should be defined in detail. When toxic materials are disposed of in underground hard rock, the contaminants will be dissolved in groundwater and moved out through the rock fracture by the flowing water in the long run. Fractures in rocks tend to dominate the water flow, when the rock matrix is of low permeability. Individual fractures act as conduits through the rock media.

There are two ways to describe the flow and migration of contaminants in fractured media: the equivalent porous medium model [Tang et al., 1981] and the fracture network model [Moreno et al., 1993]. The porous medium model characterizes hydrodynamic parameters by averaged values and has been applied to the flow in soils. When the rock mass has extremely many interconnecting fractures, the flow medium can be treated as an equivalent porous medium. Otherwise, a fracture network model will be more appropriate. The flow in the rock fracture is often assumed to be like that between two parallel and smooth plates. However, results from the laboratory and field measurements show that the parallel plate idealization does not describe adequately the fluid flow and contaminant

transport. The parallel plate model fails to recognize the spatial heterogeneity in the fracture aperture. Thus, model concepts of spatial heterogeneity have been studied by assuming variable apertures in the fracture along flow paths [Tsang et al., 1988].

As a serial work of Park et al. [1995, 2002]'s study, the progression is that of an experimental system from a simple artificial fracture to a tortuous natural fracture as well as the migration model by adding sorption and matrix diffusion terms. In this study, we are going to develop a generic model for describing the migration of tracers in various rock fractures: a variable aperture channel model for the characterization of the fracture plane and also a particle tracking scheme for the solute transport. We will present our investigations of flow and migration in two-dimensions, representing to the physical situation of the experimental setup.

TRANSPORT MODELING

1. Aperture Characterization and Flow Field in the Rock Fracture

When the flow in the fracture is assumed as a steady state flow in a confined aquifer, the transmissivity between sets of two boreholes, T , may be calculated [Bear, 1979]:

$$T = \frac{Q}{2\pi\Delta h} \ln \left[\frac{2d}{r_w} \right] \quad (1)$$

where Q is the volumetric flow rate, Δh is the hydraulic head, r_w is the radius of injection/elution borehole, and $2d$ is the distance between injection and elution boreholes.

The data obtained in the hydraulic characterization of the fracture may be used to generate an approximate distribution of the fracture aperture, b , across the block by using the standard cubic law equation [Park et al., 1997].

[†]To whom correspondence should be addressed.
E-mail: ckpark@kaeri.re.kr

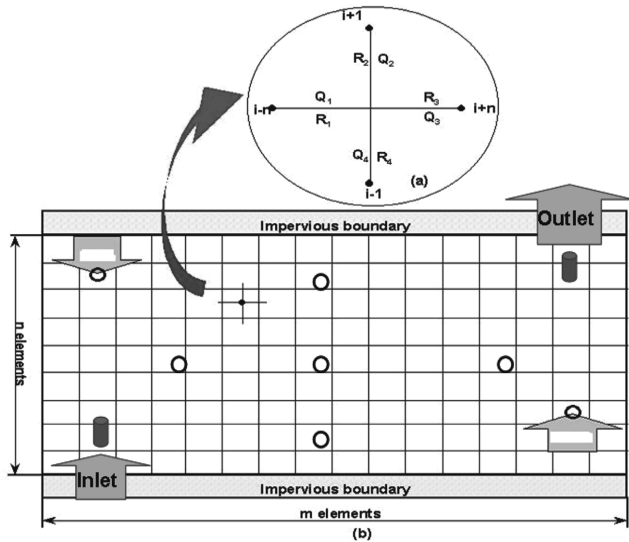


Fig. 1. Schematic diagram for the flow simulation in a subsquare in the fracture plane.

$$b = \left[\frac{12 \pi T}{\rho g} \right]^{1/3} \tag{2}$$

where μ is the viscosity of the transport solution, g is the gravitational acceleration, and ρ is the density of the transport solution.

The fracture plane may be subdivided into imaginary subsquares as shown in Fig. 1. The fluid flow through the fracture was then calculated for a constant injection/elution rate as well as for constant pressure conditions. For a constant laminar flow, the volumetric flow rate, Q_{ij} , through the subsquares enclosed by the grid lines may be written as:

$$Q_{ij} = C_{ij}(P_i - P_j) \tag{3}$$

where P_i is the pressure at node i , Node i implies an index of the i th subsquare in the fracture surface. C_{ij} is the flow conductance between nodes i and j .

The mass balance at each node may be written as:

$$\sum_j Q_{ij} = \sum_j C_{ij}(P_i - P_j) = E_i \tag{4}$$

where E_i is the injection rate or elution rate at node i . The subscript j stands for the four facing nodes of surrounding subsquares to node i . By rearranging the above equation for each node, we can obtain a system of linear equations in the form

$$[B][P] = [E] \tag{5}$$

where $[B]$ is a coefficient matrix describing the flow conductance. The matrix $[P]$ is an array describing the pressure distribution and $[E]$ is an array describing net flow rates.

Except for the nodes at the boundaries, the pressure at each node can be solved with a numerical iteration method. The flow between adjacent nodes can be calculated by using Eq. (3). After obtaining flow vectors at all nodes, solute transport can be simulated in this flow field.

2. Solute Transport Model

A two-dimensional random-walk particle tracking algorithm is

used to simulate the solute transport through the flow fields [Park et al., 1995]. Particle displacements in each time step consisted of an advective displacement based on local velocities calculated by using the pressure field and random diffusive displacement. Particles, which are representing the mass of a solute contained in a defined volume of fluid, move through a fracture with two types of motion. One motion is with the mean flow along stream lines and the other is random motion, governed by scaled probability [Desbarats, 1990]. At the inlet, a certain amount of particles were introduced and distributed at each node between flow channels with a probability proportional to the flow rates. Particles are then advected by discrete steps from node to node until they reach the outlet node at which point the arrival time is recorded. This procedure is repeated for all the particles to get a stable probability distribution. The residence time for nonsorbing tracers in a given subsquare is determined from the total flow through that subsquare and its volume. The residence time of a particle along each path is obtained as the sum of the residence times in all subsquares through which the particle has passed. Four transport processes are considered in modeling the solute transport: advection, longitudinal dispersion, diffusion into the rock mass, and sorption.

MIGRATION EXPERIMENT

The fractured granite block which has a single natural fracture of 1 m scale was sampled in a domestic quarry, through which groundwater had been flowing. This rock has an interconnected porosity of 0.37% with the specific gravity of 2.55. Fig. 2 shows the experimental setup with the granite block with dimensions of 100×60×40 (cm). The fracture is sealed with silicone rubbers when it intersects the outer surfaces of the block, and the outer surfaces are coated with the silicone too to prevent loss of groundwater by evaporation. Before the migration test, the rock blocks are submerged in the water container to be saturated with water. The water in the container kept almost a constant temperature of 20 °C. Nine boreholes were drilled in the upper block, orthogonal to and ending at the fracture surface. A flow of groundwater through the fracture between pairs of boreholes was initiated and the pressure required to maintain a steady flow was measured. These pressure values were used to calculate the transmissivity and apparent aperture of the fracture as described in Eqs. (1) & (2), respectively. Pressure transducers or concentration sensors are equipped in the boreholes and connected to the com-

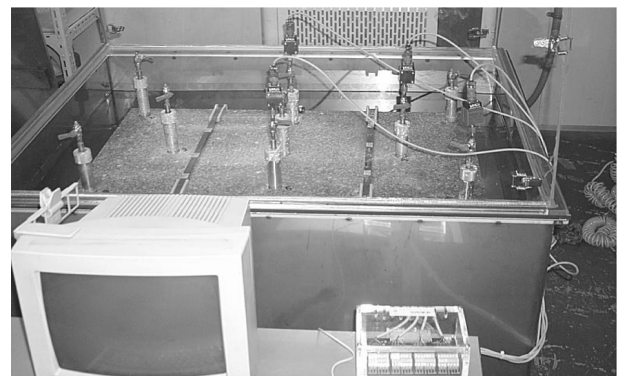


Fig. 2. The experimental setup for the migration test.

puter system to collect data as an on-line system as shown in Fig. 2.

Two boreholes on the upper plate are selected as inlet and outlet for transporting of fluid. Four kinds of chemical species are used for the migration test: (1) tritiated water (THO), (2) anions; Cl^- & Br^- (3) polymeric organic dye; NaLS (sodium lignosulfonate, $M_w=24,000$) and Eosine ($\text{C}_{20}\text{H}_6\text{Br}_4\text{Na}_2\text{O}_5$, $M_w=691$), and (4) sorbing cation; Cu^{+2} , Co^{+2} , Sr^{+2} , & Cs^+ . 1.2 ml aliquots of solution containing tracers were injected as a band input function into the inlet borehole, fed with an HPLC pump through the fracture at a flow rate of 0.2 ml/min and collected at the outlet borehole as shown in Figs. 1 & 2. The eluted solution was collected by using a fraction collector. Concentration of eosine and NaLS was analyzed with a UV/VIS spectrophotometer at the wavelengths of 524 nm, 282 nm, respectively. Concentrations of Cl^- and Br^- were analyzed with the ion electrodes of Orion Research Inc.. Sr, Co, Cu, & Cs were analyzed with an ICP-MS. THO was analyzed with a Liquid Scintillation Counter.

SIMULATION AND EXPERIMENTAL RESULTS

1. Simulation of Fracture and Flow

The fracture surface was divided into an imaginary matrix of $20 \times$

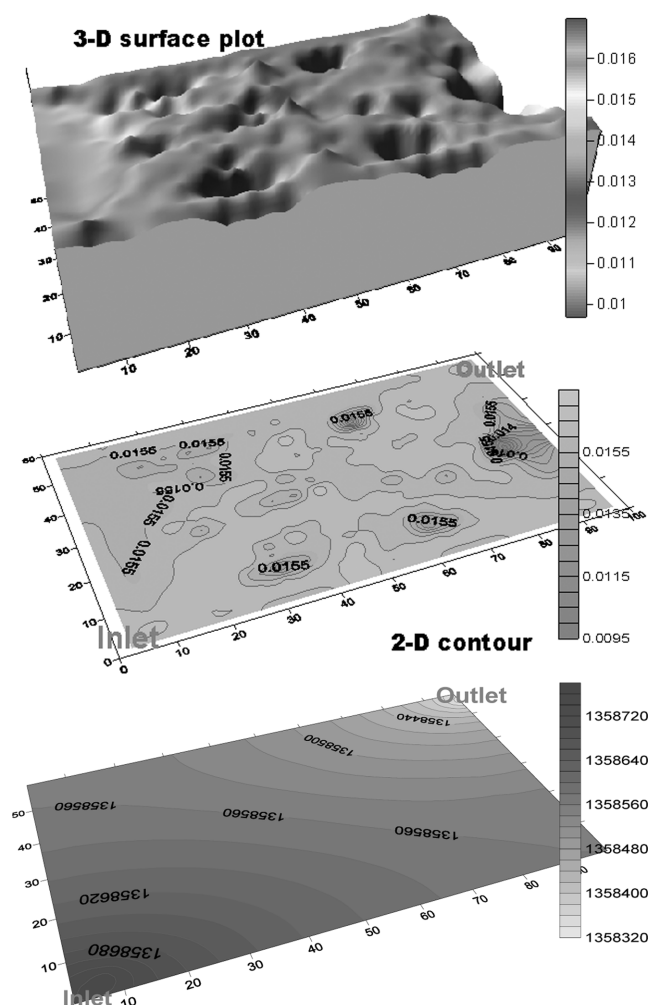


Fig. 3. Aperture plots and pressure distribution in the fracture when $Q=0.2$ ml/min.

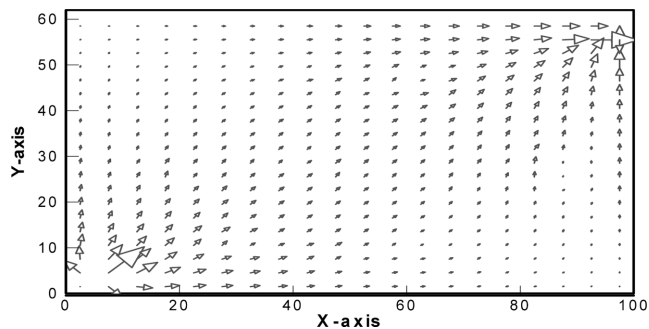


Fig. 4. Flow vector distribution in the fracture.

20 sub-squares as schematically shown in Fig. 1. The calculated results using Eqs. (1)-(5) are expressed as a two dimensional contour and a three dimensional surface plot for the aperture distribution in the fracture, and are plotted in Fig. 3. It suggests that it has a well developed fracture plane. The aperture value is distributed between 0.09 and 0.21 mm and the mean aperture value is 0.16 mm. The fracture volume is about 80 ml. Recall that the boundary conditions employed to solve the flow through the system are the constant head boundary condition, that is, the injection node is at the higher constant pressure P_1 and the elution node is at the lower constant pressure P_2 . The flow between adjacent nodes can be calculated by using Eq. (3). The pressure distribution in the field was simulated by solving the linear equations of Eq. (5) and plotted with a graphic program SURFER as shown in Fig. 3. The pressure drop, ΔP , between the inlet and the outlet was about $43,000 \text{ N/m}^2$ in the calculation. The measured pressure drop between the inlet and the outlet was about $60,000 \text{ N/m}^2$, a little higher value than the simulated.

Fig. 4 shows flow vector distribution at each node point in two dimensional flow field, which was plotted with a commercial program TECPLOT. The volumetric flow rate is represented by the size of the arrow. As already mentioned, the flow field is so well-developed that there is no significant differences of flow potentials and vectors, but, only at the edges of both sides of the fracture, the flow vectors were very small, and thus the flow was regarded as almost dead zones.

2. The Elution curves and Retardation

When a sorbing tracer moves through a fractured rock, the solute may sorb on the fracture surface. To quantify the sorption capacity, the distribution coefficient, K_a , based on the surface area is defined as

$$K_a(\text{cm}) = \frac{q_s(\text{g/cm}^2)}{C(\text{g/cm}^3)} \quad (9)$$

Where, q_s is the sorbed amount of the solute per unit specific surface area of the sorbing media, and C is the concentration of the solute in the solution.

The K_a values were measured in a static batch-type sorption experiment separately and the obtained values arranged in Table 1. The sorptive tracer may interact with the fracture surface and it retards as much as its sorption capacity. The degree of retardation is usually expressed as the retardation factor, R_f

$$R_f = \frac{\tau_n}{\tau_w} = \frac{u_w}{u_n} = 1 + \frac{K_a}{b} \quad (10)$$

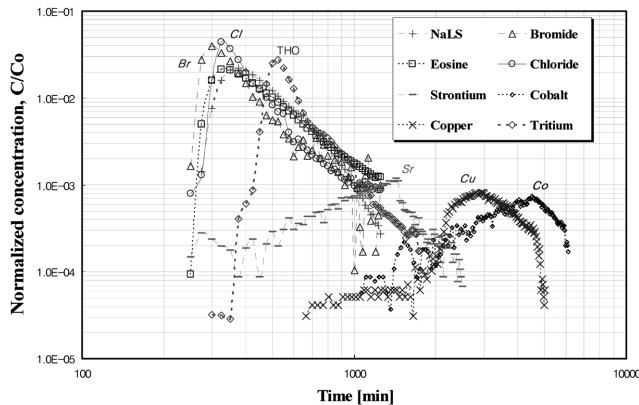


Fig. 5. Experimental elution curves of the tracers in the natural fracture.

Table 1. Results from the migration experiments

Tracer	K_a (cm) distribution coeff.	Peak arrival τ , (ml)	Recovery (%)	R_f , Retardation factor	
				Migration	Batch
Eosine	0	70	100	0.67	1.0
NaLS	0	75	99.8	0.71	1.0
Bromide	0	60	100	0.57	1.0
Chloride	0	65	100	0.62	1.0
Tritium	0	105	82.9	1.0	1.0
Strontium	0.11	285	23.8	2.71	13.
Cobalt	3.5	901	19.5	8.58	384.
Copper	9	560	21.4	5.33	322.

where τ is the transporting time, u is velocity, subscript n is tracer, w is water,

The experimental elution curves of the tracers are shown together in Fig. 5 and the data are arranged in Table 1. If the gap of the fracture is assumed as a thin cube, the average aperture of the fracture can be estimated from the elution curve of nonsorbing tracer and from the mass balance in the fracture.

$$LW(b/\tau)=Q \quad (6)$$

where, τ is peak arriving time of the elution curve. Above equation can be rearranged for the aperture as

$$b=(Q/LW)\tau \quad (7)$$

The obtained aperture value was about 0.011 cm. It gives reasonable correspondence with the simulated result of 0.016 cm based on a hydraulic test. While the mean linear velocity in the fracture is expressed as

$$u=Q/(W \cdot b) \quad (8)$$

The obtained value of u is about 0.33 cm/min.

The migration characteristics of tracers according to their chemical properties can be examined with the elution curves. In these curves, the tritiated water was regarded as a basic tracer because it has same chemical properties with water. Usually, tritium, anion, and some organic dye are assumed as the nonsorbing tracer [Moreno et al., 1985]. Therefore, in modeling work, it is commonly assumed

that the value of the distribution coefficient is zero, $K_a=0$, and the value of the retardation factor is one, $R_f=1$, for such nonsorbing tracers as arrange in Table 1. However, in this experiment, they showed a little different migration behavior. The anions and polymeric organic dyes migrate faster than the tritium in the natural fracture as compared at the R_f /migration column in Table 1. And they are recovered almost 100% at the exit, while tritium was recovered only 83%. This phenomenon can be explained as follows. Because the surface of the rock fracture is negatively charged, the anion and the negatively charged organic dye could be expelled by the rock surface and thus cannot access to the pore by the anion exclusion effect [Lanmuir, 1997]. Therefore, it could be concluded that tritium diffuses into the rock pores, but anions and polymeric tracers hardly diffuse into the rock matrix.

The elution curves of sorbing tracers such as Sr, Co, & Cu show significant retardation and dispersion phenomena. And the recovery percentages are around 20%. However, Cs did not come out but sorbed on the fracture surface tightly.

The R_f values from the elution curves of sorbing tracers compared to that of tritium are calculated and arranged at the R_f /migration column in Table 1, while R_f can also be presumed from batch sorption data by Eq. (10) and also arranged at the R_f /batch column in Table 1. The R_f values from the elution curve was smaller than those from the sorption data.

To put it concretely, the R_f of Sr is about 2.7 from the elution curve, while the predicted R_f from the sorption is roughly 12. Therefore, it can be concluded that the migration velocity is not slow enough to give sufficient contact time for sorbing on the fracture surface at the linear velocity of 0.33 cm/min. Moreover, the difference of the R_f values between from the migration and from the sorption for Sr is smaller than those for Co and Cu. It may be explained as the difference of sorption mechanism. That is, the Sr sorbs reversibly by the electrostatic force and desorbs or exchanges easily by other cations dissolved in the groundwater. On the other hand, Co and Cu sorb not only by the ion-exchange reaction but also by the selective sorption with iron-manganese oxides irreversibly. The Cs sorbs irreversibly on specific affinitive minerals like mica and so its elution can hardly be observed in the outlet [Park et al., 1999].

The natural fracture system is so heterogeneous that it is very difficult to characterize transport process quantitatively. Thus, in order to get idea from the elution curves in the fracture system, model simulation was carried out for some simple cases. The considered cases are 1) the tracer moves with solution only by advection, 2) moving by advection and sorption, 3) moving by advection and matrix-diffusion, and 4) moving by advection, sorption and matrix-diffusion. The degree of sorption was simulated by the magnitude of R_f value, and the degree of matrix-diffusion was presented by the diffusivity into the pore, D_p . Thus trends of elution curves are investigated by varying R_f and D_p values. The simulated results are fitted together with some experimental ones in Fig. 6. The larger the R_f value, the more retardation of the elution peak and the longer tail. The variation of D_p gives similar results but wider dispersion effect. Therefore, the matrix-diffusion process gives a significant retardation and dispersion effects in the migration process compared to the case of sorption-only in this flow system.

The Anion, Cl^- , fitted somewhat with the advection-only case in Fig. 6. The tritium curve shows some retardation effect and is roughly

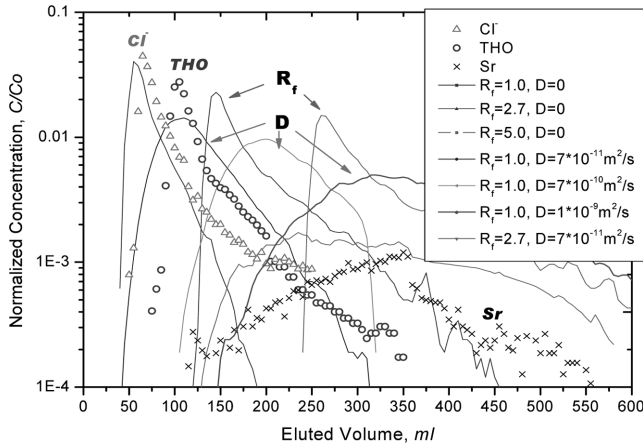


Fig. 6. Experimental and simulated elution curves of the tracers.

fitted with the case of matrix-diffusion when $D_p=7 \times 10^{-11} \text{ m}^2/\text{s}$. The roughness of the simulation curves compared to the experimental ones may have originated from the natural heterogeneity of the fracture and remaining uncertainty in the characterizing process of the field. More precision requires more disturbance of the field like the uncertainty principle. So, optimization tactics are required and nine boreholes are selected to characterize hydraulics and aperture distribution. The experimental curve of Sr implies that Sr was retarded not only by sorption but also by matrix-diffusion according to the simulation result. Usually, it is assumed that sorbing tracers are retarded only by sorption [Kinzler et al., 2003]. However, the elution curves of the sorbing tracers in this fracture system suggest matrix-diffusion and it was identified by through-diffusion experiments

[Park et al., 1992]. In the diffusion test, sorbing tracers showed unexpectedly larger diffusivities than those of nonsorbing tracers and it was explained by the surface diffusion mechanism. In the particle tracking simulation for the solute transport, the spatial distribution of the particles in the fracture at a certain time represents a migration plume. By reflecting the comparison results of the elution curves between the experimental and the simulated, the migration plumes of Sr moving from the inlet to the outlet with time are simulated when $R_f=2.7$ and $D_p=7 \times 10^{-11} \text{ m}^2/\text{s}$ and shown in Fig. 7. It shows widely dispersed plumes in the fracture plane due to sorption and matrix diffusion. At 173 ml of eluted volume, some portion of Sr plume is reached at the outlet while most of the other portion still remains in the fracture plane. Considering the experimental elution curves of Sr in Fig. 5, the elution curve appears from about 150 ml and the peak appears about 285 ml. Thus, the simulated plumes considering sorption and matrix-diffusion are in accord with the experimental elution curves.

CONCLUSIONS

The diffusion into the interconnected micropore space in rock mass has an effect on the retardation for tritium, but not for anions and polymeric substances due to anion exclusion effect. Thus, giving care to selecting a basic nonsorbing tracer would be important in estimating retardation. The retardation factor calculated from the static sorption test can easily give a higher value than that obtained from the migration test due to sorption kinetics and contact time. The matrix-diffusion process gives an effect on the retardation for sorbing tracers too and the surface diffusion is important in this process. The developed variable aperture channel model was success-

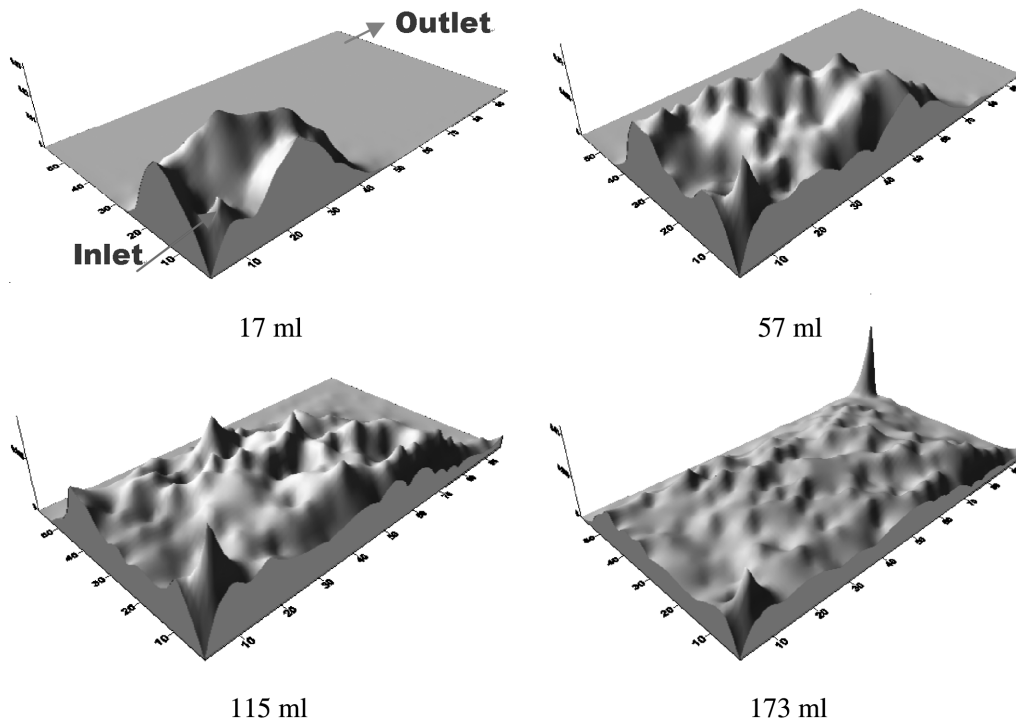


Fig. 7. Migration plumes of Sr with time in the fracture. Migration plume moves from bottom plane to the top with time. Color brightness represents concentration.

fully applied in describing the migration of the solutes in rock fractures. The combination of experimental observation and model simulation may be an effective approach to further understand the flow and transport in rock fractures.

NOMENCLATURE

- D_p : is the diffusivity into the rock pore in [m^2/s]
 Q : is the volumetric flow rate in [cm^3/sec]
 Δh : is the hydraulic head in [cm]
 r_w : is the radius of injection/elution borehole in [cm]
 $2d$: is the distance between injection and elution boreholes
 μ : is the viscosity of the transport solution in [$g/cm \cdot sec$]
 P_i : is the pressure at node i
 C : is the concentration of a solute in the solution
 C_{ij} : is the flow conductance between nodes i and j
 E_i : is the injection rate or elution rate at node i
 τ : is the transporting time (min) or peak elution volume [ml]
 u : is the linear velocity
 K_a : is the distribution coefficient based on the fracture surface area
 q_s : is the sorbed amount of a solute per the specific surface area of the sorbing media

Subscripts

- i : implies an index of the i th subsquare in the fracture surface
 j : stands for the four facing nodes of surrounding subsquares to node i

REFERENCES

- Bear, J., *Hydraulics of groundwater*, McGraw-Hill (1979).
 Desbarats, A. J., "Macrodistribution in sand-shale sequences," *Water Resour. Res.*, **26**(1), 153 (1990).
 Kinzler, B., Vejmelka, P., Römer, J., Fanghänel, Th., Wilberg, P., Jansson, M. and Eriksen, T., "Swedish-German actinide migration experiment at ÄSPÖ HRL," *Journal of Contaminant Hydrology*, **61**, 219 (2003).
 Kum, Y. S., Park, C. K., Hahn, P. S. and Choi, H. S., "An experimental study on the chemical transport through a natural rock fracture," *J. of Kor. Soc. of Env. Eng.*, **24**(8), 1479 (2002).
 Langmuir, D., *Aqueous environmental geochemistry*, Chap.3.5, Prentice-Hall (1997).
 Moreno, L., Neretnieks, I. and Eriksen, T., "Analysis of some laboratory tracer runs in natural fissures," *Water Resour. Res.*, **21**(7), 951 (1985).
 Moreno, L., Tsang, C. F., Hale, F. V. and Neretnieks, I., "Flow and tracer transport in a single fracture," *Water Res. Res.*, **24**, 2033 (1988).
 Moreno, L. and Neretnieks, I., "Flow and nuclide transport in fractured media," *J. of Contaminant Hydrology*, **13**, 49 (1993).
 Park, C. K., Park, H. H. and Woo, S. I., "Computer simulation study of transient diffusion of Cs through a granite with unsteady-state diffusion model," *J. of Nuc. Sci. Tech.*, **29**(8), 786 (1992).
 Park, C. K., Keum, D. K. and Hahn, P. S., "Stochastic analysis of contaminant transport through a rough-surfaced fracture," *Korean J. Chem. Eng.*, **12**, 428 (1995).
 Park, C. K., Vandergraaf, T. T., Drew, D. and Hahn, P. S., "Analysis of the Migration of nonsorbing tracers in a natural fractures in granite using a variable aperture channel model," *J. of Cont. Hydrol.*, **26**, 97 (1997).
 Park, C. K., Ryu, B. H. and Hahn, P. S., "Migration characteristics of some chemical species in a granite fracture according to their chemical properties," *Korean J. Chem. Eng.*, **19**, 765 (2002).
 Park, C. K. and Hahn, P. S., "Reversibility and Linearity of sorption for some cations onto a Bulguksa granite," *Korean J. Chem. Eng.*, **16**, 758 (1999).
 Tang, D. H., Friend, E. O. and Sudicky, E. A., "Contaminant transport in fractured porous media," *Water Res.*, **17**, 555 (1981).
 Tsang, Y. W., Tsang, C. F., Neretnieks, I. and Moreno, L., "Flow and tracer transport in fracture media- A variable-aperture channel model and its properties," *Water Resour. Res.*, **24**(12), (1988).
 Washburn, F. E., Kaszeta, C. S., Simmons, and Cole, C. R., "Multicomponent mass transport model," *PNL-3179* (1980).